Characterization and flocculation performance of a newly green flocculant derived from natural bagasse cellulose

Ziqiu Han[a,b,1], Jiangbo Huo[a,b,1], Xinbo Zhang[a,b,*], Huu Hao Ngo[,c,a*], Wenshan Guo[c,a], Qing Du[a,b], Yufeng Zhang[a,b], Chaocan Li[a,b], Dan Zhang[a,b]

[a]*Joint Research Centre for Protective Infrastructure Technology and Environmental Green Bioprocess, School of Environmental and Municipal Engineering, Tianjin Chengjian University, Tianjin 300384, China*

[b]*Tianjin Key Laboratory of Aquatic Science and Technology, Tianjin Chengjian University, Jinjing Road 26, Tianjin 300384, China*

[c]*Centre for Technology in Water and Wastewater, School of Civil and Environmental Engineering, University of Technology Sydney, Sydney, NSW 2007, Australia*

[1] Equal contribution

*Correspondence authors: Email: zxbcj2006@126.com (X. B. Zhang); ngohuuhao121@gmail.com (H. H. Ngo)

Abstract

A newly green natural polymer bagasse cellulose based flocculant (PBCF) was synthesized utilizing a grafting copolymerization method for effectively enhancing humic acid (HA) removal from natural water. This work aims to investigate flocculation behavior of PBCF in synthetic water containing HA, and the effects of flocculant dose and initial solution pH on flocculation performance. Results showed that PBCF functioned well at a flocculant dose of 60 mg/L and pH ranging from 6.0 to 9.0. The organic removal efficiency in synthetic water in terms of HA (UV_{254}) and chemical oxygen demand (COD_{Mn}) were up to 90.6% and 91.3%, respectively. Furthermore, the charge neutralization and adsorption bridging played important roles in HA removal. When applied for lake water, PBCF removed 91.6% turbidity and 50.0% dissolved organic matter, respectively. In short, PBCF demonstrates great potential in water treatment in a safe and environmentally friendly or 'green' way.

Keywords: Bagasse cellulose; Cationic flocculant; Flocculation behavior; Humic acid

1. Introduction

The world's supply of surface water has been severely polluted over many generations due to industrial development, rapid urbanization, rising levels of contamination, and abuse of chemical fertilizers and pesticides. Eutrophication of water bodies has worsened, and the species and quantities of organic matter in water continue to grow, leading to excessive proliferation of algae. These have ensured that the natural organic matter (NOM) content in water exceeds government standards/regulations required for drinking water sources and quality. It is estimated humus accounts for 50%-90% of natural organic matter (NOM) in water, and humic acid (HA) is an essential component of humus and dissolved organic matter (DOM) in water (Malczewska et al., 2022). HA in natural water bodies will increase the chromaticity and smell of water, and it can even form more toxic complexation with organic matter and heavy metals (Libecki et al., 2020). Moreover, HA plays a protective role for colloid particles in water by enhancing their stability, leading to challenges on how to treat water. HA can react with chlorine during chlorination to produce toxic precursors of disinfection by-products, for instance trichloromethanes which are carcinogenic and extremely harmful to human health (Lou et al., 2021).

For this reason, it is of great importance to seek effective methods to remove HA from water. To date, membrane filtration, adsorption, oxidation, biotechnology, coagulation/flocculation methods, etc., have been the subject of much attention (Du et al., 2021; Jang et al., 2021; Ryu et al., 2021; Yang et al., 2021; Zhang et al., 2021). The process of coagulation/flocculation is widely used owing to its advantages of low cost,

low energy consumption, easy operation, effective solid-liquid separation of colloidal suspension and high efficiency in removing natural organic matter from water (Wang et al., 2019).

The coagulants/flocculants for HA removal mainly include inorganic coagulants, organic polymer flocculants, and natural polymer flocculants. Of these, inorganic coagulants are widely used because they are inexpensive, yet excessive use of inorganic coagulants can introduce a lot of metal ions to water and in this way cause secondary pollution (Vereb et al., 2019). In addition, organic synthetic polymer flocculants can form stronger and denser flocs at small doses, thus increasing the rate of floc settling and obtaining better removal efficiency, whereas acrylamide is harmful to the human body (Li et al., 2017). In contrast, natural polymer flocculants are widely respected due to their environmental compatibility and renewable properties. Based on different raw materials, they can be roughly divided into five categories: chitosan flocculants, starch flocculants, lignin flocculants, plant gum flocculants and cellulose flocculants (Li et al., 2018; Chen et al., 2020b; Liu et al., 2020; Wang et al., 2021; Wu et al., 2021).

Of these, cellulose flocculants have been widely researched because their raw materials are abundant in nature. Bagasse, orange peel and pomelo peel are high in cellulose content. A large amount of bagasse wastes every year is produced by the sugar industry since sugarcane with a short growing cycle is the main cash crop grown in south China. However, bagasse is rarely reused as a resource (Ma and Wen, 2020). Therefore, the extraction of cellulose from bagasse and the utilization of cellulose can reduce the waste of resources and curb environmental pollution. As well, cellulose has

89 the advantages of porous structure and large specific surface area. The surface has a
90 large number of hydrophilic hydroxyl groups, which can provide more active sites for
91 modification. The required flocculants can be prepared by modifying cellulose and
92 introducing functional groups (Li et al., 2018). A new flocculant BPC-g-PAM was
93 prepared by grafting polyacrylamide (PAM) onto bamboo pulp cellulose (BPC) in
94 homogeneous aqueous solution (Liu et al., 2014). It can remove as much as 98% of
95 kaolin with a negative surface charge in water under acidic and neutral conditions, due
96 to the enhanced charge neutralization and bridging effect in the flocculation process. In
97 addition to good removal efficiency, it is in fact friendly to the environment. A natural
98 cellulose dicarboxylic acid flocculant (DCCs) was synthesized from dialdehyde
99 cellulose via the one-step method. It can improve the removal efficiency of kaolin and
100 papermaking wastewaters by improving neutralization in the flocculation process (Zhu
101 et al., 2015). By preparing a flocculant (CMCND) with strong cationic properties and
102 unique hydrophobic properties, CMCND demonstrated superior efficiency in removing
103 trace nonylphenol (NP), turbidity and humus from synthetic surface water (Yang et al.,
104 2016).

105 As is well known, the surface of HA in natural water is negatively charged and can
106 be removed by electro-neutralization. Therefore, by introducing cationic groups on the
107 surface of cellulose, the electrostatic repulsion and adsorption ability is enhanced.
108 Interestingly, inspired by previous research, acryloyloxyethyl trimethyl ammonium
109 chloride (DAC) is a commonly used graft monomer for quaternary amination of natural
110 polymer flocculant (Liu et al., 2019; Jiang et al., 2020). DAC can be introduced to the

bagasse cellulose surface by graft copolymerization to improve the removal of HA.

In this study, a new green flocculant namely PBCF was derived from sugarcane bagasse with potassium persulfate serving as initiator and DAC as grafting monomer. The characteristics of PBCF were analyzed, as well as the performance and mechanism of the flocculant on HA in water. This helps to explain the possibilities for improving the pretreatment process of micro-polluted water resources.

2. Materials and methods

2.1 Reagents

Bagasse was collected from the farmers' markets. Humic acid (HA) was provided by Sigma-Aldrich Corporation. DAC (80% aqueous solution) was purchased from Shanghai D&B Biological Science and Technology Co., Ltd. Meanwhile, sodium hydroxide (NaOH, AR) and potassium persulfate ($K_2S_2O_8$, AR) were purchased from Shanghai Macklin Biochemical Co., Ltd.

2.2. Preparation of PBCF

2.2.1 Preparation of alkaline bagasse cellulose

First, the bagasse purchased from the market was cleaned, soaked, and washed to remove all excess impurities. Next, the bagasse was dried until a constant weight was achieved in a 55 ℃ oven. Then, the bagasse was pulverized into 40 mesh powder for use. Following this, bagasse powder weighing 20 g was put it into a beaker, 100 mL 20% NaOH solution was added to it, and then it was soaked at room temperature for 24 h. After that, the sample was filtered and washed with distilled water until it was slightly alkaline (pH≈8.0), dried to a constant weight, and ground into powder to obtain alkaline

bagasse cellulose (Abc).

2.2.2 Preparation of PBCF

As displayed in Fig. S1, 1 g of (W_0) Abc and a specific amount of distilled water were added to a four-necked flask equipped with a gas guide and a stirring device, heated and stirred at 90 °C for one hour to allow sufficient wetting. When the temperature was reduced to the reaction temperature of 45 ℃, a certain amount of potassium persulfate (KPS) initiator was added. After it was fully dissolved, a specific mass ratio of DAC was added, and nitrogen was passed to ensure the reaction could proceed under nitrogen protection; the reaction was stopped after 3 h at 45 ℃. After the reaction finished, the product was precipitated with anhydrous ethanol, washed with anhydrous ethanol and distilled water, respectively, and dried in an oven until constant weight (W_2) was achieved. Each sample was prepared three times in duplicate. The synthesis line of the PBCF is shown in Fig. S2.

2.2.3 Determination of grafting percentage of PBCF

The grafting percentage (G) is the percentage of the mass of DAC monomer that has been grafted onto Abc to the mass of alkaline bagasse cellulose monomer. It determines the level of reaction according to the effective number of monomers in the grafting reaction (Chen et al., 2020c). It can be calculated using the following equation:

$$G = [(W_2 - W_0)/W_0] \times 100\%$$

Where W_0 denotes the initial weight of Abc, and W_2 stands for the weight of PBCF after the reaction.

154 **2.3 Raw water and coagulation experiment**

155 200 mg HA and 0.4 g sodium hydroxide were dissolved in deionized water and
156 then stirred. After the HA was dissolved, the solution was transferred to a 1.0 L
157 volumetric flask with a constant volume. The reserve solution was stored in a brown
158 reagent bottle, while the HA solution was diluted to 5 mg/L, 10 mg/L and 15 mg/L with
159 deionized water when used, and the pH of the solution was adjusted near to neutral. The
160 lake water sample was taken from the central lake at Tianjin Chengjian University
161 (Xiqing District, Tianjin). The pH, turbidity, DOM (UV_{254}), and COD of the lake water
162 are 8.0 - 9.0, 31.2 - 33.4 NTU, 6.6 - 6.9 mg/L, and 12.1 - 12.8 mg/L, respectively.

163 The flocculation process of PBCF was as follows: adding flocculant, stirring at a
164 speed of 200 r/min for 1 min, stirring at a speed of 100 r/min for 10 min, stirring at a
165 speed of 30 r/min for 20 min, left to precipitate for 40 min, taking supernatant and
166 finally, UV_{254} (DOM concentration) and COD_{Mn} were measured. Three parallel
167 samples were set up for each set of experiments.

168 **2.4 Characterization of PBCF**

169 The functional groups and surface composition of PBCF were characterized by
170 Fourier transform infrared (FT-IR) (Nicolet iS10, Thermo Fisher Technology Co., Ltd.)
171 and X-ray photoelectron spectroscopy (XPS) ((K-alpha, Thermo Scientific). The
172 surface morphology of PBCF was analyzed using a scanning electron microscope
173 (SEM) (JSM-7800F, Japan Electronics Co., Ltd.). The crystal structure of PBCF was
174 investigated by X-ray diffractometer (XRD) (D8 ADVANCE, Bruker, Germany). The
175 zeta potential of PBCF at different pH values was measured using a zeta potential

analyzer (Nano-ZS, Malvern Company, UK).

2.5 Flocculation performance analysis

Organic concentration of water samples before and after coagulation was measured in terms of UV_{254} and COD using UV-visible spectrophotometer (UV-2600, Shimadzu, Japan) and COD_{Mn} analyzer (Q-COD_{MN}, Qing Shi Jie, Shanghai), respectively. This served to determine the flocculant efficiency in removing HA. Furthermore, Zeta potential analyzer (Nano-ZS, Malvern Company, UK) measured the change in the zeta potential of water bodies before and after flocculation, while Optical flocculation tester (IPDA-100, ECONOVEL, South Korea) estimated the change in extent of flocculation during the flocculation process. On the basis of these analyses, the flocculating mechanism of the PBCF in the flocculation process was explored.

3. Results and discussion

3.1 Optimization of the flocculant preparation process

The PBCF cationic cellulose-based grafting flocculant was optimized by changing the KPS dosage and mass ratio of Abc to DAC, with the removal effect of 5 mg/L HA solution and the grafting rate of flocculant as evaluation indices.

3.1.1 Effect of KPS dosage

As shown in Fig. S3a, when the KPS dosage increased the removal efficiencies of HA by PBCF also increased firstly but then diminished. When the dosage of KPS was 1.8 g, the removal efficiency of HA reached a maximum of 90.5±0.41%. As the KPS dosage rose further, the removal efficiency of HA gradually declined. This was because KPS can stimulate hydroxyl groups on basic cellulose and enable them to provide more

active sites for graft copolymerization. However, when the dosage of KPS was too high and exceeded 1.8 g, the reaction rate occurred too rapidly, resulting in the implosion reaction between Abc and DAC (Chen et al., 2021). That caused an increase in the monomer mass and graft rate after the reaction; nevertheless, it was not conducive to the growth of the chain and generation of graft polymer (Chen et al., 2020c). Subsequently, this led to waning HA removal efficiency.

Meanwhile, the DAC copolymer adhered to the Abc surface and covered the pores and tentacle-like structures on Abc. It reduced the bridging adsorption of PBCF in the flocculation process. This was the main reason why the grafting rate of PBCF increased while the UV_{254} removal rate fell when the amount of KPS was more than 1.8 g.

3.1.2 Effect of m (Abc): m (DAC)

The influence of the mass ratio of Abc on DAC regarding HA removal and graft rate is depicted in Fig. S3b. It can be seen that as the ratio of m (Abc) to m (DAC) increased gradually, the rate of removing 5 mg/L HA by PBCF flocculant increased first but then decreased. When m (Abc): m (DAC) was 1:3, the maximum HA removal rate can reach up to 90.5±0.41%. With the increase in the DAC ratio, the positive charge on the polymer chain rose and thus the electric neutralization effect of flocculant was enhanced, which helped flocculation sedimentation. However, when the proportion of DAC in the reaction system was too large, it caused too much of a positive charge on the polymer chain. As a result, the remaining positive charge reversed the properties of the particle surface charge and augmented the repulsive force between the particles. This led to the repulsive force between the flocculant and the colloidal particles and

reduction of the flocculation effect. Moreover, excessive DAC gave rise to self-polymerization, and increased the grafting of PBCF first and then decreased slowly.

3.2 Characterization of PBCF

3.2.1 Scanning electron microscope

The SEM images of Abc, PBCF showed obvious structural changes (Fig 1). After soaking in NaOH solution, the surface of alkaline bagasse cellulose was noticeably etched (Fig. 1a). According to the yellow area shown in Fig. 1b, the surface of Abc is coarse with a large number of wrinkles and pores. This unique structure provided suitable conditions for the graft copolymerization reaction (Fig. 1a and b). However, the product surface (PBCF) looked smoother, and many protrusions on the surface of PBCF can be observed (Fig. 1c and d). Observations suggested that this surface showed abundant lamellar and fiber-like structures, which could undoubtedly increase the surface area of the product. In this way, it would be more conducive to boosting the adsorption and bridging effect and enhancing removal of colloidal particles in the flocculation (Fig. 1e and f).

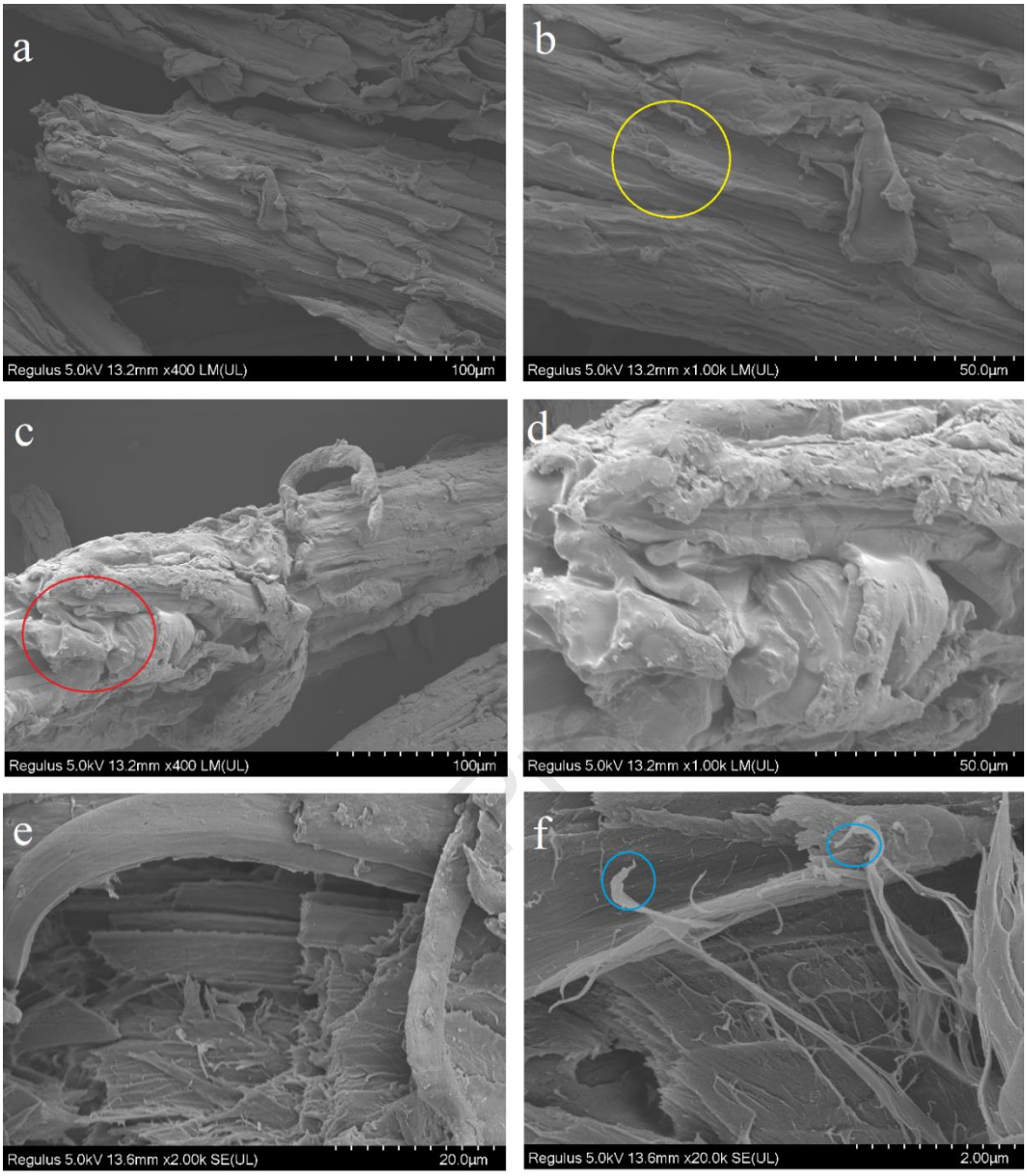

Fig. 1. SEM micrographs of Abc (a, b) and PBCF (c, d, e, f)

3.2.2 Fourier transform infrared

Fig. 2a indicated that the absorptive peaks of Abc at 3442 cm^{-1}, 2915 cm^{-1}, 1391 cm^{-1} and 1049 cm^{-1} could be assignable to O-H stretching vibration, C-H symmetric stretching vibration, C-H bending vibration, and -CH stretching vibration on cellulose skeleton, respectively (Jiang et al., 2020; Tang et al., 2020). The band at 1644 cm^{-1} was attributed to OH bending vibration in absorbed water. Apart from the original

characteristic peaks of Abc, some new absorption peaks at 1282 cm^{-1} and 1736 cm^{-1} emerged in PBCF, which belonged to the stretching vibration of C-N, and COOR, respectively (Wang et al., 2019). The absorption peaks at 1049 cm^{-1} were significantly enhanced. This is caused by the reaction of DAC with the -OH on the cellulose skeleton, resulting in a stretching vibration of -CH (Liu et al., 2019; Tang et al., 2021). Generally, structural changes confirmed that the DAC monomer was successfully grafted onto the Abc molecular chain.

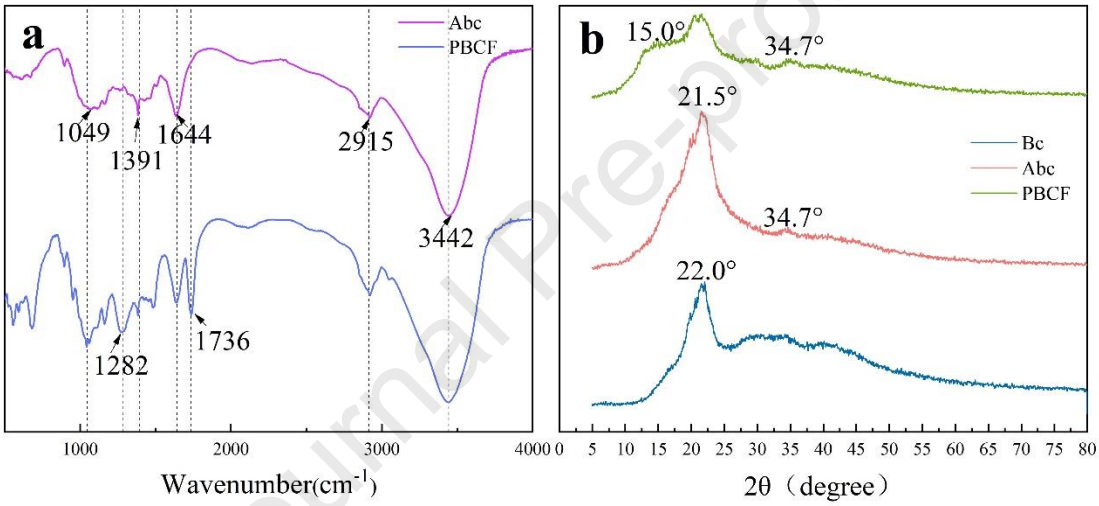

Fig. 2. (a) FTIR of Abc and PBCF; (b), XRD of Bc, Abc, and PBCF

3.2.3 X-ray diffraction

The crystal structures of bagasse cellulose, alkaline bagasse cellulose, and PBCF were characterized by XRD. The XRD spectra of Bc, Abc, and PBCF are shown in Fig. 2b. A wide peak appeared at 2θ = 22°, which belonged to the crystallization peak of natural cellulose Ⅰ (Badawy et al., 2021). The XRD spectrum of Abc showed that the characteristic peak of Bc shifted to 21° from 22° and a small diffraction peak appeared at 2θ = 34.7°, which matched well with the crystal structure of cellulose Ⅰβ (Tewatia et al., 2021). The diffraction peak intensity of Abc at 2θ = 21.5° increased, and the

crystallinity reduced from 86.89% to 65.74%, meaning that the glycosidic bonds and molecular chains of network structure in Bc after NaOH treatment gradually broke up (Rizwan et al., 2021). Due to the hydrolysis of the amorphous regions of cellulose, the hydrogen bonds among molecular chains of cellulose were severely broken. Amorphous regions and disordered crystals were further destroyed, whereas the regular crystals did not change, thus crystallinity of Abc decreased. Based on this, PBCF exhibited a small diffraction peak at 15° and the crystallinity was 75.1%. This suggested that DAC was successfully grafted onto Abc, which greatly reduced the hydrogen bonding of cellulose and changed the original structure.

3.2.4 X-ray photoelectron spectroscopy

XPS analysis further confirmed that the DAC monomer was successfully grafted to the alkaline bagasse cellulose monomer. The XPS full scan spectra of Abc and PBCF are shown in Fig. 3. The PBCF contained C, O, N, and S, while Abc contained only C and O and less N. The peak of PBCF at 402.5 eV is the characteristic peak of N1s quaternary ammonium salt derived from DAC (Liu et al., 2017). The main elements C 1s and O 1s of Abc and PBCF were analyzed. Through the spectra of C 1s and O 1s, it emerged that C-O, C-OH and C-H were transformed into O-C=O and C-N through a graft copolymerization reaction, resulting in more O-C=O and C-N. It strongly proved the occurrence of graft copolymerization (Liu et al., 2019).

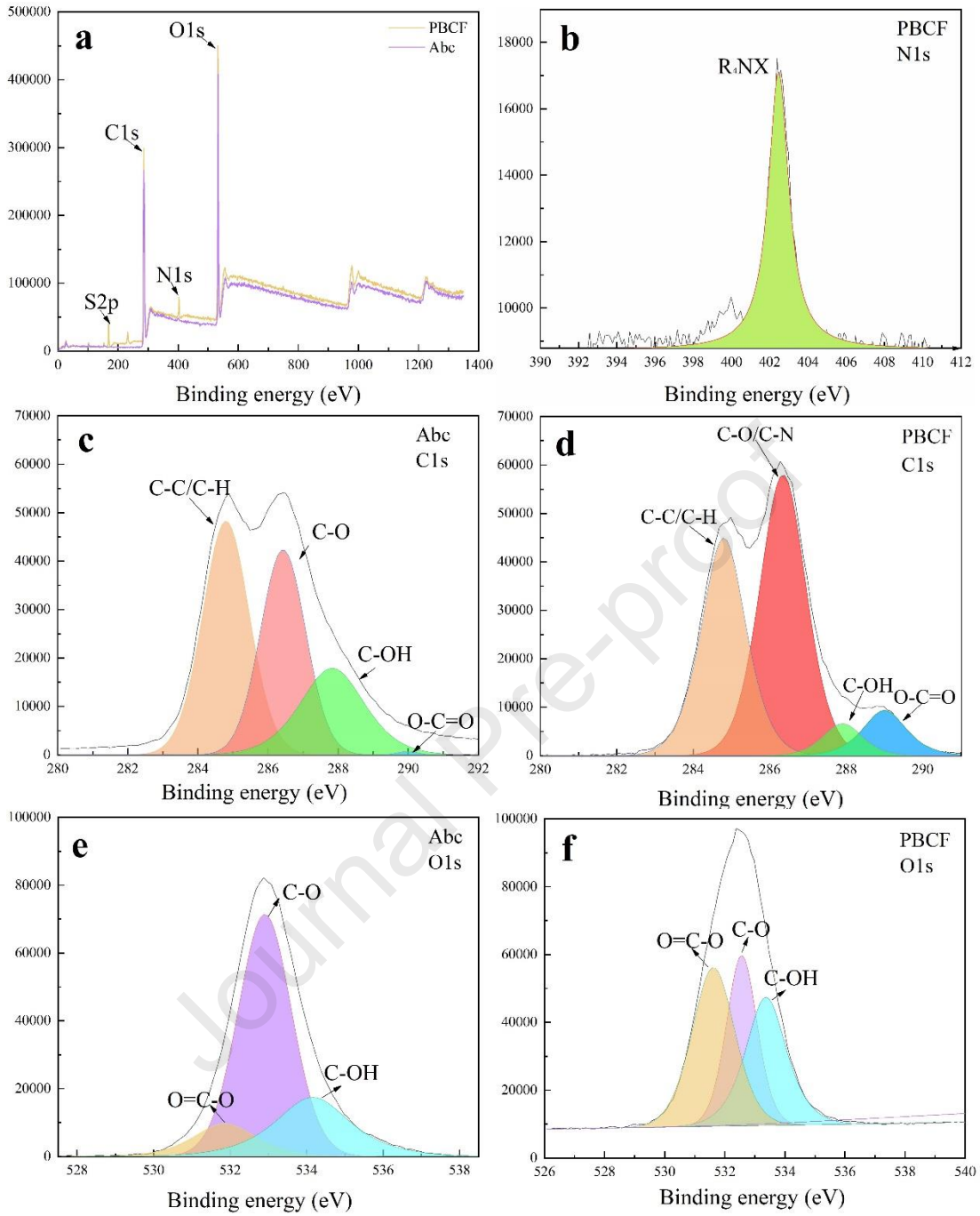

Fig. 3. XPS of Abc (a, c, e) and PBCF (a, b, d, f)

3.2.5 Zeta potential

The zeta potentials of BPCF at different pH values are exhibited in Fig. S4. As shown in Fig. S4, the PBCF exhibited a positive charge at pH ranging from 3 to 10. In addition, the zeta potential of PBCF presented a decrease trend, which was resulted from the restricted ionization of the quaternary amine group on the PBCF molecular

chain under alkaline conditions (Kuncoro et al., 2018a; Kuncoro et al., 2018b). This allowed the PBCF to provide good removal of HA in a wide pH range.

3.3 Flocculation of synthetic water

3.3.1 Effect of flocculant dose

The flocculant dose plays a decisive role in water treatment, and the optimized dose can ensure the rational utility of resources. In this study, flocculation performance was investigated in the simulated synthetic water with pH of 7 at 25 ℃. As displayed in Fig. 4a, removal rates of organic matter based UV_{254} and COD_{Mn} rapidly increased and then decreased. When the dose of PBCF was up to 60.0 mg/L, removal rates of UV_{254} and COD_{Mn} reached the maxima of 90.57±0.41% and 91.33±1.15%, respectively. However, when the PBCF dose continued increasing, the removal rate abated gradually. This phenomenon can be attributed to the adsorption charge neutralization in the flocculation process (Ma et al., 2021).

Changes in the zeta potential and Flocculation Index (FI) values in the flocculation process are depicted in Fig. 4b and c. The flocculation appearance time t_1 gradually decreased when the PBCF dose increased (Fig. 4c). When the dose of PBCF was 80 mg/L, t_1 was minimal at 720 s. However, due to the overdosing of flocculant, repulsion between flocs occurred, causing the flocs decomposed quickly. In addition, the value of FI would gradually increase when the flocs were aggregated, and therefore the higher value of FI caused the larger floc particle size. The floc particle size reached its maximum value at the PBCF dosage of 60 mg/L. t_2 and the corresponding time required were smallest at the flocculant dose of 50 mg/L. This proved that the coagulation rate

was at its largest when the flocculant dose was 50 mg/L. When the flocculant dose was greater than 60 mg/L, the zeta potential gradually tended to stabilize.

It proved that when the dose of PBCF was less than 50 mg/L, electrical neutralization tended to dominate the flocculation process. At this time, the floc size was small and the removal effect was poor. When the flocculant dose increased continuously, the adsorption bridging capacity was gradually enhanced and took the leading role. When the dose of PBCF was beyond 70 mg/L, the flocculant proved to be excessive, leading to a repulsive interaction among the flocculant molecules. Thus, the adsorption bridging interaction gradually weakened, gradually shrinking the floc size and the removal performance as well. It can be seen that the adsorption bridging effect of PBCF played a dominant role in removals of UV_{254} and COD_{Mn}. The size of the formed floc was largest when PBCF dose was 60 mg/L, under which the as-prepared PBCF exhibited the best HA removal performance.

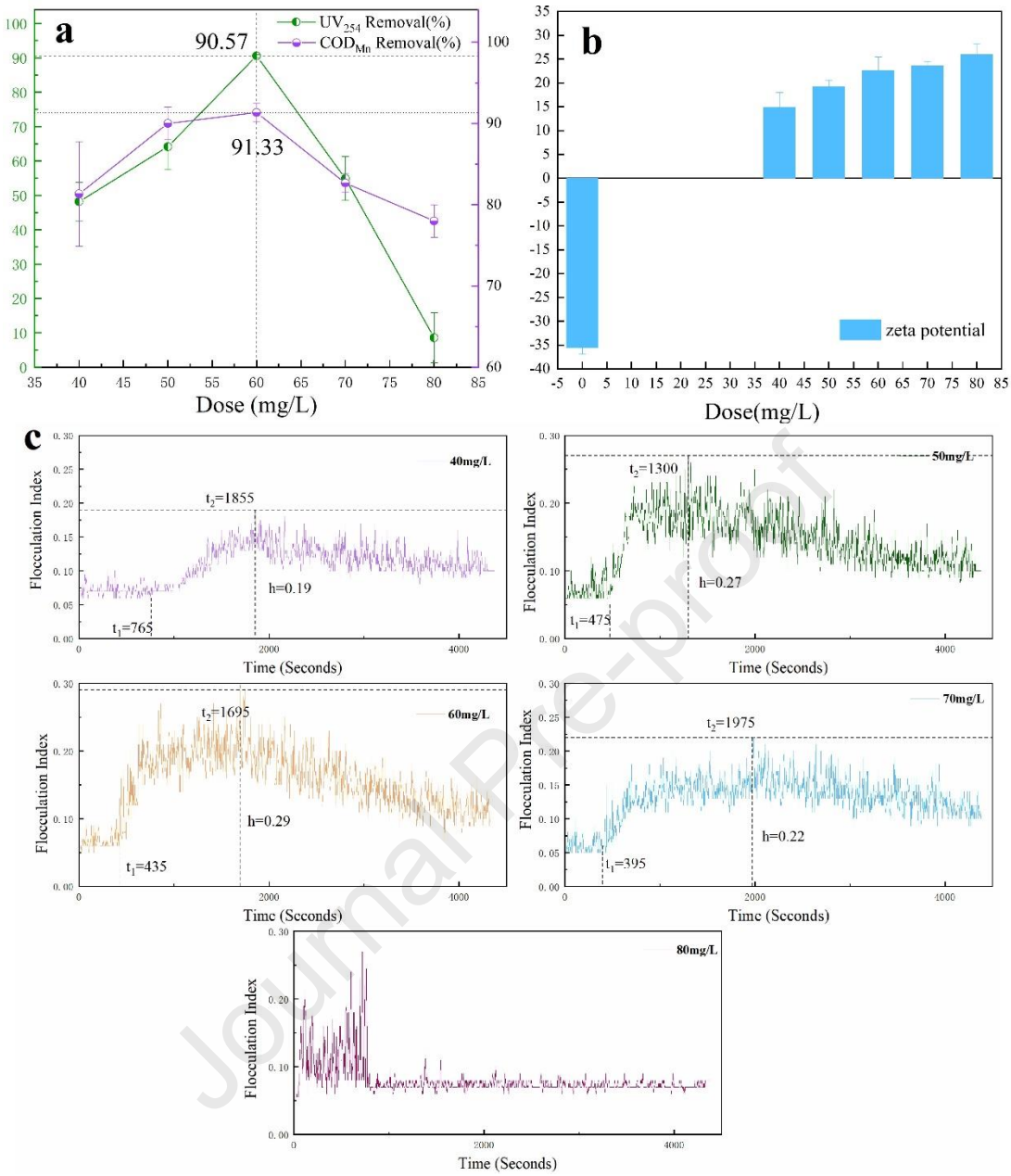

Fig. 4. Effects of dose on removal efficiencies (a) of UV_{254}, COD_{Mn}, zeta potential (b), and Flocculation Index (c) (h and t_2 represent the final size of flocs and the time when the floc size reaches the maximum value, respectively)

3.3.2 Effects of pH

The effect of synthetic water pH at 4.0 – 10.0 was examined at a dose of 60.0 mg/L of PBCF, as shown in Fig. 5. As can be seen from Fig. 5a, the removal efficiencies of UV_{254} and COD_{Mn} were improved as pH increased from 4.0 to 7.0. The best UV_{254} and

329 COD_{Mn} removals reached the maximum value of 90.57±0.41% and 91.33±1.15%,
330 respectively, at pH of 7.0. When the pH level was more than 7.0, the removal rate
331 decreased slightly with an increase in the pH. This was mainly due to the protonation
332 and deprotonation of HA at different pH (Liu et al., 2020). At a low pH, it was difficult
333 for protons to depart from HA, which made HA more stable in water. Moreover, the
334 surface of PBCF was positively charged. Since the electrical neutralization effect
335 weakened during the flocculation process, it was hard to remove HA under acidic
336 conditions. In addition to HA protonation, functional groups belonging to the
337 carboxylic or phenolic acids of the HA group would be more likely to deprotonate at
338 higher pH, which resulted in more charges on the HA surface. This could be explained
339 by the fact of poor removal efficiency of PBCF for UV_{254} and COD_{Mn} in the acid range.
340 Fig. 5b shows the changes occurring in zeta potential before and after flocculation.
341 Due to the protonation of HA and the interaction of PBCF, the colloidal particles in
342 water experienced a charge reversal behavior. The colloidal suspension appeared to be
343 stable when the pH changed from 4.0 to 6.0. When pH was about 8.0, the zeta potential
344 of the supernatant after flocculation was close to 0 mV, and the removal efficiency
345 diminished when the pH increased. It is evidence that charge neutralization and
346 adsorption bridging both existed in the flocculation. With the increase of pH, more
347 negative charges of HA would be electrically neutralized with PBCF, and the degree of
348 deprotonation of HA would be reinforced. Furthermore, the number of flocculants used
349 for adsorption bridge would be reduced.
350

The small flocs generated by adsorption charge neutralization cannot form large flocs by effective collision. This also led to the poor removal of dissolved organic matter. Fine flocs cannot easily settle but they can be filtered through a filter membrane which is 0.45 μm in size.

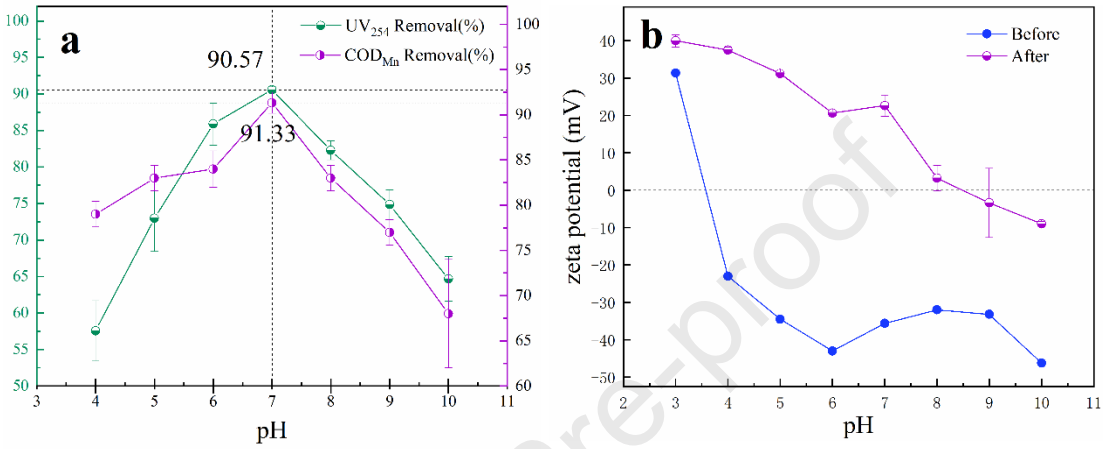

Fig. 5. Effects of pH on (a) removal efficiencies of UV_{254}, COD_{Mn} (b) zeta potential of water before and after flocculation.

3.3.3 Effects of initial HA concentrations

As shown in Fig. S5a and b, when the HA concentration was 10 mg/L, the maximum removal rates of UV_{254} and COD_{Mn} were 94.03±0.65% and 88.00±1.41%, respectively, at the dose of PBCF of 80 mg/L. With the increase of PBCF dose, the removal rate gradually improved. When the HA concentration was 15 mg/L, the UV_{254} removal rate reached the highest (94.11±0.40%) at the dose of PBCF of 80 mg/L. When the dosage was more than 80 mg/L, the UV_{254} removal rate gradually stabilized to more than 92.52%. At the PBCF dose of 70 mg/L, the maximum removal rate of COD_{Mn} amounted to 90.67±0.47%. With the gradual increase of the PBCF dose, the removal rate fell slightly.

Combined with the changes in zeta potential of the PBCF before and after flocculation (Fig. S5b), it can be seen that as the zeta potential of the supernatant gradually approached the isoelectric point, the efficiency of the flocculant in removing HA gradually increased, presenting a positive correlation trend. A slight decrease was observed when the zeta potential became positive.

When the HA solution was 10 mg/L, and the dose of flocculant was 80 mg/L, the adsorption bridging ability of the flocculant was not fully utilized. Therefore, with the increase in the flocculant mass, the simulated water exhibited strong positive electricity. The flocculant repelled and this in turn reduced the removal efficiency. However, when the concentration of HA increased to 15 mg/L, the adsorption bridging capacity was fully utilized, and the simulated water presented weak positive electricity. Consequently, the removal efficiency tended to be stable.

Under the same conditions, the flocculant's effectiveness in removing large concentrations of HA was not significantly reduced. This is mainly due to a dominant role of PBCF in adsorption bridging throughout the HA removal process. With the increase of HA concentration, the collision probability of flocculant and HA in solution was greatly strengthened. The number of colloidal particles produced after flocculation rose. In the flocculation stage the colloid particles constantly collided, which elevated the volume of flocs. With the rising number of alum blooms, the settling speed became faster and the removal efficiency improved.

3.4 Flocculation of lake water

3.4.1 Dose optimization

Taking turbidity, UV_{254}, and COD_{Mn} removal rates as indices, the influence of PBCF dosage on coagulation performance in natural lake water was investigated. The flocculant dosage of 60 mg/L achieved the best removal efficiency for turbidity with residual turbidity of only 2.79±0.03 NTU and a removal rate of 91.61±0.09%. When the dose of PBCF was 40 mg/L, the efficiencies in removing UV_{254} and COD_{Mn} reached the maximum of 48.08±0.34% and 51.27±0.71%, respectively. However, both amounts were smaller than the best removal efficiency in synthetic water (Fig. 6a and b).

This phenomenon indicated that the turbidity removal efficiency by PBCF is better than that of UV_{254} and COD_{Mn}. This is mainly because insoluble colloidal particles in water were more easily removed by coagulation compared with DOM. Additionally, it was gradually enhanced with the increase of flocculant dose but nevertheless, the repulsive force appeared when too much flocculant was added to the water sample. This led to the gradual decline in UV_{254} and COD_{Mn} removal. No other pollutants were added to the synthetic water, allowing the flocculant to target HA for removal so better removal efficiencies of UV_{254} and COD_{Mn} were obtained. It is important to note that the insoluble colloidal particles in water would combine with these particles formed by flocculation, triggering an in increase in colloidal particles weight and more conducive conditions for the removal of the remaining turbidity in water.

PBCF can effectively remove turbidity, UV_{254} and COD_{Mn} from lake water. Sugarcane bagasse is cheap and readily available compared to other biomass, which

considers a renewable resource while the PBCF preparation process does not cause secondary pollution to the environment. Moreover, the sludge floc formed by flocculation is small in size, which facilitates its application in practical engineering(Chen et al., 2020a).

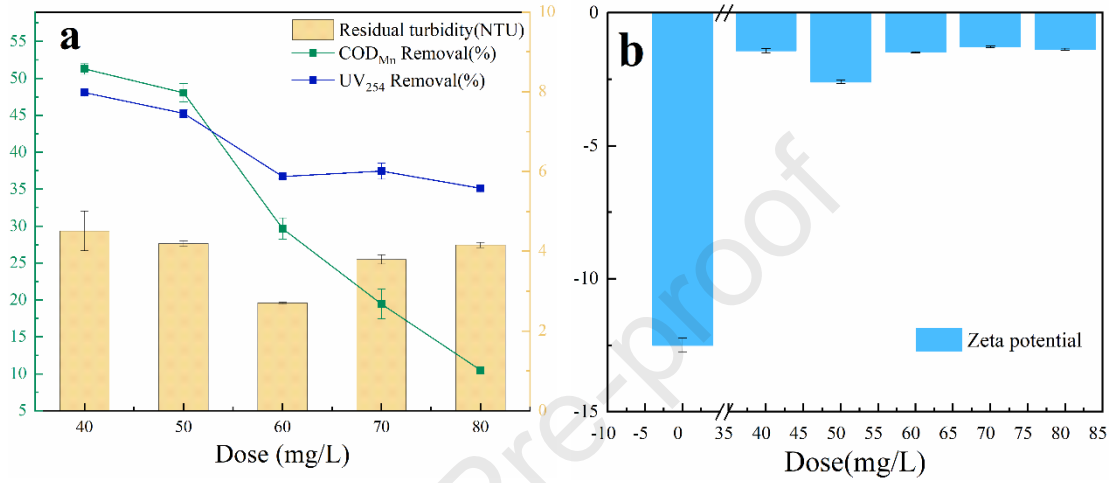

Fig. 6. Effects of dose of (a) PBCF on removal efficiencies of UV_{254}, COD_{Mn}, and residual turbidity (b) zeta potential.

3.4.2 Three-dimensional fluorescence analysis.

Fluorescence spectrophotometer (LS55, USA PE) was implemented to conduct three-dimensional fluorescence analysis on water samples before and after treatment. The PBCF's effectiveness was further explored for treating DOM in lake water. The EEM spectra were divided into five regions, which represented separately the different compositions of organic compounds in water before and after coagulation (Chen et al., 2003). In general, regions I and II represent aromatic proteins; region III stands for fulvic acids; and regions IV and V are related to soluble microbial by-products and HA, respectively.

Fig. 7 showed that after coagulation, the concentration of organic compounds in

the supernatant of zones III, IV, and V decreased significantly, and the concentrations of organic compounds in zones I and II fell slightly. This outcome indicated that PBCF was very efficient in removing xanthogenic acid and HA organic compounds, whereas it exhibited poor removal efficiency of aromatic protein organic compounds. The main reason for this situation is the high molecular weight of fulvic acid and HA etc. (regions III, IV and V), which readily charge neutralization and bridging with PBCF. Nevertheless, the aromatic proteins (regions I and II) are stable due to the presence of their own benzene ring structure. Therefore, they are not easily removed (Loganathan et al., 2020; Tian et al., 2020).

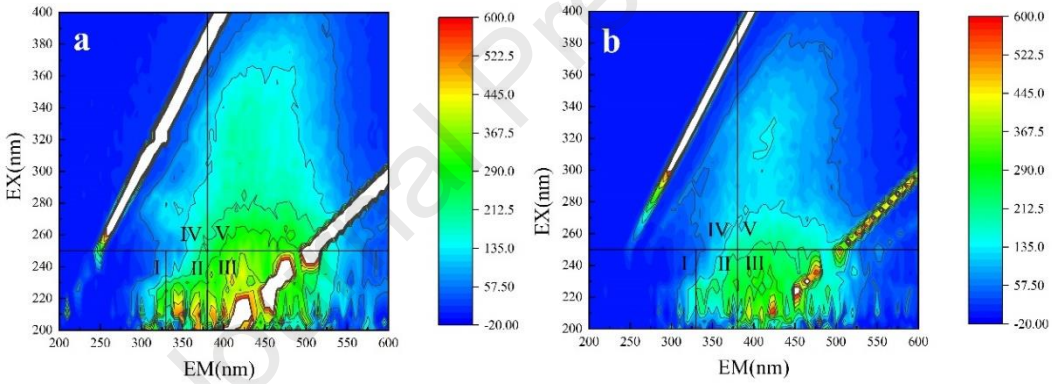

Fig. 7. (a) EEM of lake water before and (b) after treatment by PBCF

4. Conclusions

A newly green flocculant (PBCF) was derived from natural polymer bagasse cellulose. PBCF exhibited excellent performance in removing HA from water. It was found that adsorption bridging and electric neutralization played a key role in removing HA. Remarkably, PBCF can effectively reduce DOM and turbidity in natural lake water via adsorption bridging interaction. Overall, this will offer a substitute flocculant for water pretreatment and new insights into the flocculating process.

Acknowledgements

This research was supported by Tianjin Municipal Science and Technology Bureau of China (Project No. 18PTZWHZ00140, 20JCZDJC00380) and TG Hilyte Environment Technology (Beijing) Co., LTD. (Project No. M-P-0-181001-001).

References

Badawy, A.A., Ghanem, A.F., Yassin, M.A., Youssef, A.M., Abdel Rehim, M.H., 2021. Utilization and characterization of cellulose nanocrystals decorated with silver and zinc oxide nanoparticles for removal of lead ion from wastewater. Environmental Nanotechnology, Monitoring & Management 16,115735.

Chen, F., Liu, W., Pan, Z., Wang, Y., Guo, X., Sun, S., Jia, R., 2020a. Characteristics and mechanism of chitosan in flocculation for water coagulation in the Yellow River diversion reservoir. Journal of Water Process Engineering 34,101191.

Chen, M., Zou, C., Tang, W., Huang, Y., Sun, H., 2021. Characterization and flocculation evaluation of a new organic–inorganic hybrid polymer flocculant (PAC - AM - DMC). Journal of Applied Polymer Science 138,51388.

Chen, N., Liu, W., Huang, J., Qiu, X., 2020b. Preparation of octopus-like lignin-grafted cationic polyacrylamide flocculant and its application for water flocculation. Int J Biol Macromol 146, 9-17.

Chen, W., Westerhoff, P., Leenheer, J.A., Booksh, K., 2003. Fluorescence Excitation−Emission Matrix Regional Integration to Quantify Spectra for Dissolved Organic Matter. Environmental Science & Technology 37, 5701-5710.

Chen, X., Wang, D., Wang, S., Song, H., Gu, Q., Zhang, Y., 2020c. Synthesis and

Dewatering Properties of Cellulose Derivative-Grafting DMC Amphoteric Biodegradable Flocculants. Journal of Polymers and the Environment 29, 565-575.

Du, T., Zhang, G., Zou, J., 2021. Coupling photocatalytic and electrocatalytic oxidation towards simultaneous removal of humic acid and ammonia-nitrogen in landscape water. Chemosphere 286, 131717.

Jang, H., Park, S.J., Kim, J., 2021. Response surface methodology to investigate the effects of operational parameters on membrane fouling and organic matter rejection in hard-shell encased hollow-fiber membrane. Chemosphere 287, 132132.

Jiang, X., Lou, C., Hua, F., Deng, H., Tian, X., 2020. Cellulose nanocrystals-based flocculants for high-speed and high-efficiency decolorization of colored effluents. Journal of Cleaner Production 251,119749.

Kuncoro, E.P., Isnadina, D.R.M., Darmokoesoemo, H., Fauziah, O.R., Kusuma, H.S., 2018a. Characterization, kinetic, and isotherm data for adsorption of Pb2+ from aqueous solution by adsorbent from mixture of bagasse-bentonite. Data in Brief 16, 622-629.

Kuncoro, E.P., Mitha Isnadina, D.R., Darmokoesoemo, H., Dzembarahmatiny, F., Kusuma, H.S., 2018b. Characterization and isotherm data for adsorption of Cd(2+) from aqueous solution by adsorbent from mixture of bagasse-bentonite. Data Brief 16, 354-360.

Li, M., Wang, Y., Hou, X., Wan, X., Xiao, H.-N., 2018. DMC-grafted cellulose as green-based flocculants for agglomerating fine kaolin particles. Green Energy & Environment 3, 138-146.

Li, X., Zheng, H., Wang, Y., Sun, Y., Xu, B., Zhao, C., 2017. Fabricating an enhanced

sterilization chitosan-based flocculants: Synthesis, characterization, evaluation of sterilization and flocculation. Chemical Engineering Journal 319, 119-130.

Libecki, B., Kalinowski, S., Wardzyńska, R., Bęś, A., 2020. Using an angular detection photometer (ADP) in analyzing the humic acids coagulation process. Journal of Water Process Engineering 37,101507.

Liu, C., Gao, B., Wang, S., Guo, K., Shen, X., Yue, Q., Xu, X., 2020. Synthesis, characterization and flocculation performance of a novel sodium alginate-based flocculant. Carbohydr Polym 248, 116790.

Liu, H., Yang, X., Zhang, Y., Zhu, H., Yao, J., 2014. Flocculation characteristics of polyacrylamide grafted cellulose from Phyllostachys heterocycla: An efficient and eco-friendly flocculant. Water Res 59, 165-171.

Liu, T., Ding, E., Xue, F., 2017. Polyacrylamide and poly(N,N-dimethylacrylamide) grafted cellulose nanocrystals as efficient flocculants for kaolin suspension. Int J Biol Macromol 103, 1107-1112.

Liu, Y., Zheng, H., An, Y., Ren, J., Zheng, X., Zhao, C., Zhang, S., 2019. Ultrasound-assisted synthesis of the β-cyclodextrin based cationic polymeric flocculants and evaluation of flocculation performance: Role of β-cyclodextrin. Separation and Purification Technology 228,115735.

Loganathan, P., Gradzielski, M., Bustamante, H., Vigneswaran, S., 2020. Progress, challenges, and opportunities in enhancing NOM flocculation using chemically modified chitosan: a review towards future development. Environmental Science: Water Research & Technology 6, 45-61.

Lou, J., Lu, H., Wang, W., Zhu, L., 2021. Molecular composition of halobenzoquinone

514 precursors in natural organic matter in source water. Water Res 209, 117901.

515 Ma, J., Xia, W., Zhang, R., Ding, L., Kong, Y., Zhang, H., Fu, K., 2021. Flocculation of
516 emulsified oily wastewater by using functional grafting modified chitosan: The
517 effect of cationic and hydrophobic structure. Journal of Hazardous Materials
518 403,123690.

519 Ma, X., Wen, G., 2020. Development history and synthesis of super-absorbent polymers:
520 a review. Journal of Polymer Research 27, 136.

521 Malczewska, B., Farnood, R.R., Tabe, S., 2022. Natural organic matter removal by
522 electrospun nanofiber membranes coated with heated aluminum oxide particles.
523 Journal of Water Process Engineering 45,102498.

524 Rizwan, M., Gilani, S.R., Durrani, A.I., Naseem, S., 2021. Low temperature green
525 extraction of Acer platanoides cellulose using nitrogen protected microwave
526 assisted extraction (NPMAE) technique. Carbohydr Polym 272, 118465.

527 Ryu, J., Jung, J., Park, K., Song, W., Choi, B., Kweon, J., 2021. Humic acid removal and
528 microbial community function in membrane bioreactor. J Hazard Mater 417,
529 126088.

530 Tang, F., Yu, H., Yassin Hussain Abdalkarim, S., Sun, J., Fan, X., Li, Y., Zhou, Y., Chiu
531 Tam, K., 2020. Green acid-free hydrolysis of wasted pomelo peel to produce
532 carboxylated cellulose nanofibers with super absorption/flocculation ability for
533 environmental remediation materials. Chemical Engineering Journal 395,125070.

534 Tang, Q., Chen, W., Dai, X., Liu, Y., Liu, H., Fan, L., Luo, H., Ji, L., Zhang, K., 2021.
535 Exploring the perspective of nano-TiO2 in hydrophobic modified cationic
536 flocculant preparation: Reaction kinetics and emulsified oil removal performance.

Chemosphere 263, 128066.

Tewatia, P., Kaur, M., Singhal, S., Kaushik, A., 2021. Wheat straw cellulose based fluorescent probe cum bioadsorbents for selective and sensitive alleviation of uranium(VI) in waste water. Journal of Environmental Chemical Engineering 9,106106.

Tian, Z., Zhang, L., Sang, X., Shi, G., Ni, C., 2020. Preparation and flocculation performance study of a novel amphoteric alginate flocculant. Journal of Physics and Chemistry of Solids 141,109408.

Vereb, G., Gayir, V.E., Santos, E.N., Fazekas, A., Kertesz, S., Hodur, C., Laszlo, Z., 2019. Purification of real car wash wastewater with complex coagulation/flocculation methods using polyaluminum chloride, polyelectrolyte, clay mineral and cationic surfactant. Water Sci Technol 80, 1902-1909.

Wang, M., Feng, L., You, X., Zheng, H., 2021. Effect of fine structure of chitosan-based flocculants on the flocculation of bentonite and humic acid: Evaluation and modeling. Chemosphere 264, 128525.

Wang, Z., Huang, W., Yang, G., Liu, Y., Liu, S., 2019. Preparation of cellulose-base amphoteric flocculant and its application in the treatment of wastewater. Carbohydr Polym 215, 179-188.

Wu, Y., Jiang, X., Ma, J., Wen, J., Liu, S., Liu, H., Zheng, H., 2021. Low-pressure UV-initiated synthesis of cationic starch-based flocculant with high flocculation performance. Carbohydr Polym 273, 118379.

Yang, H., Zheng, X., Zhang, D., Tang, G., Li, X., Wu, H., Yan, W., Zhi, H., 2021. Comparison of the effect of PANI/TiO2, Dow resins and activated carbon in

removing model dissolved organic matter (DOM) and phosphorus. Journal of Water Process Engineering 43,102302.

Yang, Z., Ren, K., Guibal, E., Jia, S., Shen, J., Zhang, X., Yang, W., 2016. Removal of trace nonylphenol from water in the coexistence of suspended inorganic particles and NOMs by using a cellulose-based flocculant. Chemosphere 161, 482-490.

Zhang, H., Lin, H., Li, Q., Cheng, C., Shen, H., Zhang, Z., Zhang, Z., Wang, H., 2021. Removal of refractory organics in wastewater by coagulation/flocculation with green chlorine-free coagulants. Sci Total Environ 787, 147654.

Zhu, H., Zhang, Y., Yang, X., Liu, H., Shao, L., Zhang, X., Yao, J., 2015. One-step green synthesis of non-hazardous dicarboxyl cellulose flocculant and its flocculation activity evaluation. J Hazard Mater 296, 1-8.

Highlights

- A cationic flocculant (PBCF) was prepared for using agricultural waste as a resource.
- PBCF was effective in removing HA at different concentrations.
- PBCF is highly efficient for UV_{254}, COD_{Mn} and turbidity in lake water.
- Dose-pH graphs and correlation analyses confirmed flocculation during HA removal.
- Electrical neutralization and adsorption bridging dominated HA removal.